

## Journal Pre-proofs

Design, synthesis, and biological evaluation of novel dual PPAR $\alpha/\delta$  agonists for the treatment of T2DM

Qiang Ren, Liming Deng, Zongtao Zhou, Xuekun Wang, Lijun Hu, Rongrong Xie, Zheng Li

PII: S0045-2068(20)30455-7  
DOI: <https://doi.org/10.1016/j.bioorg.2020.103963>  
Reference: YBIOO 103963

To appear in: *Bioorganic Chemistry*

Received Date: 26 February 2020  
Revised Date: 2 May 2020  
Accepted Date: 20 May 2020

Please cite this article as: Q. Ren, L. Deng, Z. Zhou, X. Wang, L. Hu, R. Xie, Z. Li, Design, synthesis, and biological evaluation of novel dual PPAR $\alpha/\delta$  agonists for the treatment of T2DM, *Bioorganic Chemistry* (2020), doi: <https://doi.org/10.1016/j.bioorg.2020.103963>

This is a PDF file of an article that has undergone enhancements after acceptance, such as the addition of a cover page and metadata, and formatting for readability, but it is not yet the definitive version of record. This version will undergo additional copyediting, typesetting and review before it is published in its final form, but we are providing this version to give early visibility of the article. Please note that, during the production process, errors may be discovered which could affect the content, and all legal disclaimers that apply to the journal pertain.

© 2020 Published by Elsevier Inc.



## Design, synthesis, and biological evaluation of novel dual PPAR $\alpha$ / $\delta$ agonists for the treatment of T2DM

Qiang Ren<sup>1, 2</sup>, Liming Deng<sup>1</sup>, Zongtao Zhou<sup>1</sup>, Xuekun Wang<sup>3</sup>, Lijun Hu<sup>1</sup>, Rongrong Xie<sup>1\*</sup>, Zheng Li<sup>1, 2\*</sup>

<sup>1</sup> School of Pharmacy, Guangdong Pharmaceutical University, Guangzhou 510006, PR China.

<sup>2</sup> Key Laboratory of New Drug Discovery and Evaluation, Guangdong Pharmaceutical University, Guangzhou 510006, PR China.

<sup>3</sup> College of pharmacy, Liaocheng University, Liaocheng 252059, China.

### Abstract

Dual PPAR $\alpha$ / $\delta$  agonists have been considered as potential therapeutics for the treatment of type 2 diabetes mellitus. After comprehensive structure-activity relationship study based on GFT505, a novel dual PPAR $\alpha$ / $\delta$  agonist compound **6** was identified with highly activities on PPAR $\alpha$ / $\delta$  and higher selectivity against PPAR $\gamma$  than that of GFT505. The modeling study revealed that compound **6** binds well to the binding pockets of PPAR $\alpha$  and PPAR $\delta$ , which formed multiple hydrogen bonds with key residues related to the activation of PPAR $\alpha$  and PPAR $\delta$ . Moreover, oral glucose tolerance test exhibited that compound **6** exerts dose-dependent anti-diabetic effects in *ob/ob* mice and reveals similar potency to that of GFT505, the most advanced candidate in this field. These findings suggested that compound **6** is a promising candidate for further researches, and the extended chemical space might help us to explore better PPAR $\alpha$ / $\delta$  agonist.

**Keywords:** Dual agonist; PPAR; T2DM; GFT505; Selectivity.

### 1. Introduction

Type 2 diabetes mellitus (T2DM), known as a progressive metabolic disorder, is characterized by elevated levels of blood glucose due to relatively insufficient insulin secretion and resistance [1, 2]. If blood glucose of type 2 diabetic patients cannot be effectively controlled, it may cause a

---

\* Corresponding author.

E-mail addresses: li.zheng.sky@163.com (Z. Li), happyyuyun\_1985@126.com (R. Xie).

consequence of chronic complications, such as retinopathy, renal disease, heart disease, hypertension and peripheral vascular disease [3]. Currently, the continuing emergence of the insufficient potency, hypoglycemia, and gastrointestinal side effects, motivates the search for novel anti-diabetic drugs, especially for the multi-target drugs [4-7].

The peroxisome proliferator-activated receptors (PPARs) belong to the nuclear receptor superfamily as a class of ligand-inducible transcription factors. The crucial roles in glucose and lipid metabolism make it possible for PPARs to become drug targets for T2MD and a series of metabolic syndrome [8-10]. PPARs can be subdivided into three subtypes including PPAR $\alpha$ , PPAR $\delta$  and PPAR $\gamma$ . Each subtype is pharmacologically distinct in that they are encoded separately, and the residues sequence is various at the ligand-binding site [11, 12]. The activation of PPAR $\alpha$  not only decrease triglyceride and increase HDL cholesterol but also stabilizes glucose homeostasis and ameliorates insulin resistance [13-15]. Therefore, PPAR $\alpha$  agonists have been widely used for hyperlipidemia in clinical trials, such as fenofibrate (**Figure 1**) [16]. In addition to improving dyslipidemia, the activation of PPAR $\delta$  can increase insulin sensitivity and thereby synergized with PPAR $\alpha$  for the treatment of T2DM [17-21]. In previous researches, we have identified several PPAR $\delta$  agonists with great potential on glucolipid metabolism [22-26]. The pharmacological role of PPAR $\gamma$  is associated with adipogenesis, lipid storage, and glucose homeostasis [27]. Over the years, PPAR $\gamma$  (rosiglitazone) and dual PPAR $\alpha/\gamma$  (ragaglitazar) agonists (**Figure 1**) have been developed to treat T2DM [28-30]. However, further research on this series of agonists is prevented by multiple adverse effects related to PPAR $\gamma$ , including weight gain, fluid reaction, hemodilution, and edema effect [31, 32]. Therefore, the development of dual PPAR $\alpha/\delta$  agonists with minimum activity on PPAR $\gamma$  might be provided a better benefit/risk ratio for the treatment of T2DM.

GFT505 (**Figure 1**) is a dual PPAR $\alpha/\delta$  agonist, and the selectivity against PPAR $\gamma$  is still to be improved. Furthermore, no literature has been reported to disclose the structure-activity relationship (SAR) of GFT505. In this study, we carried out SAR study on the three parts of GFT505 (**Figure 2**) and finally got compound **6** with higher selectivity to PPAR $\alpha/\delta$  and low agonistic activity on PPAR $\gamma$ . Moreover, compound **6** revealed dose-dependent hypoglycemic effects in the oral glucose tolerance test *in vivo*.

## 2. Results and discussion

## 2.1 Chemistry

The synthetic route for compounds **1-10** is depicted in **Scheme 1**. Initial, compounds **1a-1c** are etherified with iodides under basic conditions by classical Williamson ether synthesis. These ethers and thioethers (**2a-2d** and **4a**) are subsequently aldol-condensed with a series of *p*-hydroxybenzaldehyde derivatives under the catalysis of sulfuric acid to obtain intermediates **3a-3f** and **5a**. Finally, these phenolic hydroxyl intermediates and bromo alkyl methyl ester combined under heating and basic by Williamson ether synthesis, and then hydrolysis at room temperature using lithium hydroxide monohydrate as a catalyst to provide target compounds **1-10**.

## 2.2 SAR study

GFT505, a typical PPARs agonist, consists of three parts: a carboxylic acid head, a lipophilic tail, and a linker. In this study, we tried to modify the three parts of GFT505 to clarify the SAR, and to obtain more promising dual PPAR $\alpha/\delta$  agonist (**Figure 2**). *In vitro* activities data for all compounds are listed in **Table 1**. First, GFT505 was replaced methylthio with methoxy and introducing fluoro at R<sub>6</sub>-position led to compound **1**, whose potency is 1.5 fold higher to PPAR $\gamma$  and approximately half lower to PPAR $\alpha/\delta$  than GFT505. Modifying the lipophilic tail to 2,3-dihydrobenzofuran (compound **4**) gave the same trend as compound **1** on potency to PPARs. The potency of compound **4** is further increased on PPAR $\gamma$  and reduced on PPAR $\alpha/\delta$ . Substituting the methoxy of compound **1** by deuteration and deuterated methylthio provided compounds **2** and **3**, are reduced potency on PPAR $\gamma$  compared to compound **1**. Among compounds **1-4**, compound **3** has the best agonistic effect on PPAR $\alpha/\delta$ , while the agonistic activity on PPAR $\alpha/\delta$  is still lower than GFT505. These modifications at the lipophilic tail are not conducive to enhancing the agonistic activity of PPAR $\alpha/\delta$  and have little effect on the agonistic activity of PPAR $\gamma$ .

Next, we try to modify the benzene ring at the right hand side. Interestingly, mono-substitution of the right hand benzene ring with halogen provided compound **5** (fluorine) and **6** (chlorine), which almost completely loss the agonistic effect on PPAR $\gamma$  while maintaining great potency on PPAR $\alpha/\delta$ . Among them, the potency of chlorine substitution (compound **6**) is better than that of fluorine substitution (compound **5**). Based on compound **6**, we continue to modify the substituents at the alpha position of the carboxylic acid. The results show that the more methyl substituents at the alpha position of the carboxylic acid of these compounds (compound **6** vs **8** and **9**), the better potency on

PPAR $\alpha/\delta$ . Similar to the above findings, it is also shown that two methyl groups at the alpha position of the carboxylic acid are essential for the potency of PPARs (compound **5** vs **7**, GFT505 vs compound **10**). Therefore, we conducted further research on the optimal compound **6** based on its considerable potencies on PPAR $\alpha/\delta$  and better selectivity against PPAR $\gamma$  (PPAR $\alpha$  EC<sub>50</sub> = 0.468  $\mu$ M, PPAR $\delta$  EC<sub>50</sub> = 0.362  $\mu$ M and PPAR $\gamma$  > 10  $\mu$ M).

### 2.3 Molecular docking study

As shown in **Figure 3**, the binding pocket of PPAR $\alpha$  and PPAR $\delta$  are a Y-shaped cavity with three arms, and compound **6** can bind well to these two binding pockets with a similar binding pattern. Compound **6** occupies arm-I and arm-II regions in these both of Y-shaped cavities. In the arm-I region, carboxylic acid head of compound **6** forms hydrogen bonds with TYR-314, HIS-440 and TYR-464 at PPAR $\alpha$ , and HIS-323, HIS-449 and TYR-473 at PPAR $\delta$ . Two methyl substituents at the alpha position of the carboxylic acid are located on the hydrophobic region and form indispensable hydrophobic interaction with hydrophobic residue. The hydrophobic interaction may be crucial for the agonistic potency of PPAR $\alpha$  and PPAR $\delta$  [33-35]. Because, in the SAR study, when there are no two methyl groups, the potency on PPAR $\alpha/\delta$  is reduced by 6-fold compared to the presence of two methyl groups. Moreover, the chlorine substituent points to arm-III region but is not inserted, and can form a hydrophobic interaction with adjacent hydrophobic residues in the binding pocket of PPAR $\alpha$  and PPAR $\delta$ . Under the same conditions, the hydrophobicity of the chlorine substituent is slightly stronger than fluorine substituent, which explains that the potency of compound **6** on PPAR $\alpha/\delta$  is slightly better than compound **5** *in vitro* activities data. However, there is a difference. The conformation of compound **6** in the binding pocket of PPAR $\delta$  is U-shaped, but in the binding pocket of PPAR $\alpha$ , compound **6** is twisted into S-shaped due to hydrogen bonding with THR-283.

### 2.4 Oral glucose tolerance test

The hypoglycemic effect of compound **6** was evaluated by oral glucose tolerance test *in vivo* in *ob/ob* mice. During the oral glucose tolerance test, compound **6** revealed dose-dependent hypoglycemic effects after five days treatment (**Figure 4**). Moreover, the hypoglycemic effect of compound **6** is equivalently to that of GFT505 (10mg/kg), and is slightly better in compound **6**

group at the dose of 20mg/kg. These results indicated that compound **6** might be a potential candidate as effective as GFT505 *in vivo*, despite lower potencies of compound **6** on PPARs compared to GFT505 *in vitro*.

### 3. Conclusion

A novel dual PPAR $\alpha$ / $\delta$  agonist was discovered through the SAR study of GFT505. Compound **6** is a highly potent PPAR $\alpha$ / $\delta$  agonist (PPAR $\alpha$  EC<sub>50</sub>: 0.468  $\mu$ M, PPAR $\delta$  EC<sub>50</sub>: 0.362  $\mu$ M), and its selectivity against PPAR $\gamma$  (PPAR $\gamma$  EC<sub>50</sub> > 10  $\mu$ M) is better than that of GFT505. Moreover, molecular docking study shows that compound **6** binds well to the binding pockets of PPAR $\alpha$  and PPAR $\delta$  and can form multiple hydrogen bonds with key residues related to the activation of PPAR $\alpha$  and PPAR $\delta$ . During oral glucose tolerance test, compound **6** exerts dose-dependent anti-diabetic effects in *ob/ob* mice and reveals similar potency to that of GFT505. In summary, we described the SAR study based on the modification of GFT505, and compound **6** was identified as a promising candidate for further researches.

### 4. Experimental section

#### 4.1 General Chemistry

All reagents solvents were purchased from commercial sources and used as received without further purification. Normal phase column chromatography was carried out on silica gel (200-300 mesh), and TLC analysis was carried out on GF254 plates. NMR spectra were recorded in DMSO-d<sub>6</sub> on a Bruker ACF-300Q, and chemical shifts are calibrated internal tetramethylsilane standard. Mass spectrometry was performed on liquid chromatography-tandem mass spectrometry (Waters) equipped with electrospray ionization (ESI) probe. Melting points were measured by RY-1 melting-point apparatus.

#### General synthetic procedure for intermediates **2a-d**

To a solution of **1a-c** (1 equiv) in acetonitrile was added K<sub>2</sub>CO<sub>3</sub> (3 equiv), and trideuterio(iodo)methane (3 equiv). The mixture was stirred at room temperature for 12h. The mixture was filtered and the filtrates were concentrated to **2a-d**.

**General synthetic procedure for intermediates 3a-c and 5a**

**2a-c** (or **4a**) (1 equiv) and 4-hydroxy-3,5-dimethylbenzaldehyde (or 4-hydroxybenzaldehyde) (1 equiv) were dissolved in MeOH, and H<sub>2</sub>SO<sub>4</sub> (0.05 equiv) was added dropwise to the mixture. The mixture was stirred at room temperature for 16h. The solution was concentrated to give the crude product. Water (20 mL) was added to the crude product and extracted with ethyl acetate (3×10mL). After the solvent was concentrated under reduced pressure, it was purified by column chromatography to afford to **3a-c** (or **5a**).

**General synthetic procedure for intermediates 3d-f**

**2d** (1 equiv) and 3-Fluoro-4-hydroxybenzaldehyde (3-Chloro-4-hydroxybenzaldehyde or 4-Hydroxy-3-methylbenzaldehyde) (1 equiv) were dissolved in MeOH, and H<sub>2</sub>SO<sub>4</sub> (0.05 equiv) was added dropwise to the mixture. The mixture was stirred at room temperature for 16h. The solution was concentrated to give the crude product. Water (20 mL) was added to the crude product and extracted with ethyl acetate (3×10 mL). After the solvent was concentrated under reduced pressure, it was purified by column chromatography to afford to **3d** (**3e** or **3f**).

**(E)-3-(3-chloro-4-hydroxyphenyl)-1-(4-(methylthio)phenyl)prop-2-en-1-one (3e)**

<sup>1</sup>H NMR (300 MHz, DMSO-*d*<sub>6</sub>)  $\delta$ : 10.84 (s, 1H), 8.11 (d, *J* = 8.3 Hz, 2H), 8.04 (s, 1H), 7.95 – 7.75 (m, 1H), 7.72 – 7.55 (m, 2H), 7.39 (d, *J* = 8.3 Hz, 2H), 7.02 (d, *J* = 8.3 Hz, 1H), 2.56 (s, 3H).

**General synthetic procedure for targets 1-6**

To a solution of **3a-e** (or **5a**) in acetonitrile was added K<sub>2</sub>CO<sub>3</sub> (3 equiv), and methyl 2-bromo-2-methylpropanoate (1.1 equiv). The mixture was stirred at room temperature for 12h. The mixture was filtered and the filtrate was concentrated to afford solid. The residue was purified by silica gel column chromatography to afford a white solid, which was dissolved in the mixed solvent of THF/MeOH/H<sub>2</sub>O (18 mL, 2:3:1), and added lithium hydroxide (1.5 equiv). After stirring at room temperature for 4 h, the volatiles were removed under reduced pressure. The residue was acidified with 1N hydrochloric acid solution and then filtered and the filter cake was washed with cold water (5 mL), dried in vacuum to afford a white powder. Recrystallization from 75% ethanol provides pure compound **1-6**.

**(E)-2-(4-(3-(3-fluoro-4-methoxyphenyl)-3-oxoprop-1-en-1-yl)-2,6-dimethylphenoxy)-2-methylpropanoic acid (1)**

Yield 45%; m.p. 123-125 °C; <sup>1</sup>H NMR (300 MHz, DMSO-*d*<sub>6</sub>) δ: 13.00 (s, 1H), 8.23 – 8.00 (m, 2H), 7.83 (d, *J* = 15.5 Hz, 1H), 7.69 – 7.53 (m, 3H), 7.31 (t, *J* = 8.4 Hz, 1H), 3.95 (s, 3H), 2.22 (s, 6H), 1.38 (s, 6H). <sup>13</sup>C NMR (75 MHz, DMSO-*d*<sub>6</sub>) δ: 188.12 (C15), 176.35 (C1), 155.25 (C5), 153.09 (C19), 152.63 (C18), 144.68 (C13), 131.85 (C16), 130.58 (C8), 130.43 (C21), 129.38 (C20), 128.65 (C7, C9), 126.34 (C6, C10), 121.49 (C14), 115.73 (C17), 81.53 (C2), 55.87 (C22), 25.68 (C3, C4), 18.12 (C11, C12). (The carbon numbers of the compound use the default atom numbers in Chemdraw.) ESI-MS *m/z*: 385.1 [M-H]<sup>-</sup>. Anal. calcd. For C<sub>22</sub>H<sub>23</sub>FO<sub>5</sub>: C, 68.38; H, 6.00; Found: C, 68.23; H, 6.15.

**(E)-2-(4-(3-(3-fluoro-4-(methoxy-d3)phenyl)-3-oxoprop-1-en-1-yl)-2,6-dimethylphenoxy)-2-methylpropanoic acid (2)**

Yield 38%; m.p. 125-127 °C; <sup>1</sup>H NMR (300 MHz, DMSO-*d*<sub>6</sub>) δ: 12.93 (s, 1H), 8.16 – 7.94 (m, 2H), 7.84 (d, *J* = 15.0 Hz, 1H), 7.68 – 7.51 (m, 3H), 7.41 – 7.21 (m, 1H), 2.23 (s, 6H), 1.39 (s, 6H). <sup>13</sup>C NMR (75 MHz, DMSO-*d*<sub>6</sub>) δ: 187.79 (C15), 176.21 (C1), 155.43 (C5), 153.16 (C19), 152.67 (C18), 144.65 (C13), 131.86 (C16), 130.76 (C8), 130.52 (C21), 129.43 (C20), 128.76 (C7, C9), 126.38 (C6, C10), 121.46 (C14), 114.86 (C17), 81.53 (C2), 25.65 (C3, C4), 18.07 (C11, C12). ESI-MS *m/z*: 388.1 [M-H]<sup>-</sup>. Anal. calcd. For C<sub>22</sub>H<sub>20</sub>D<sub>3</sub>FO<sub>5</sub>: C, 67.85; H, 6.73; Found: C, 67.68; H, 6.79.

**(E)-2-(4-(3-(3-fluoro-4-((methyl-d3)thio)phenyl)-3-oxoprop-1-en-1-yl)-2,6-dimethylphenoxy)-2-methylpropanoic acid (3)**

Yield 42%; m.p. 128-130 °C; <sup>1</sup>H NMR (300 MHz, DMSO-*d*<sub>6</sub>) δ 8.03 (dd, *J* = 8.2, 1.8 Hz, 1H), 7.97 (dd, *J* = 11.3, 1.8 Hz, 1H), 7.82 (d, *J* = 15.5 Hz, 1H), 7.66 (d, *J* = 15.5 Hz, 1H), 7.55 (s, 2H), 7.53 – 7.45 (m, 1H), 2.27 (s, 6H), 1.34 (s, 6H). <sup>13</sup>C NMR (75 MHz, DMSO-*d*<sub>6</sub>) δ: 188.13 (C15), 179.25 (C1), 160.58 (C18), 153.25 (C5), 145.18 (C13), 135.29 (C16), 132.65 (C19), 128.19 (C20), 126.33 (C8), 124.58 (C7, C9, C21), 124.43 (C6, C10), 121.37 (C14), 114.92 (C17), 81.55 (C2), 25.63 (C3, C4), 18.05 (C11, C12). ESI-MS *m/z*: 404.1 [M-H]<sup>-</sup>. Anal. calcd. For C<sub>22</sub>H<sub>20</sub>D<sub>3</sub>FO<sub>4</sub>S: C, 65.16; H, 6.46; Found: C, 65.03; H, 6.32.

**(E)-2-(4-(3-(2,3-dihydrobenzofuran-5-yl)-3-oxoprop-1-en-1-yl)-2,6-dimethylphenoxy)-2-methylpropanoic acid (4)**

Yield 49%; m.p. 148-150 °C; <sup>1</sup>H NMR (300 MHz, DMSO-*d*<sub>6</sub>) δ: 8.14 – 7.94 (m, 2H), 7.81 (d, *J* = 15.5 Hz, 1H), 7.63 – 7.43 (m, 3H), 6.90 (d, *J* = 8.4 Hz, 1H), 4.66 (t, *J* = 8.8 Hz, 2H), 3.27 (t, *J* = 8.8 Hz, 2H), 2.23 (s, 6H), 1.38 (s, 6H). <sup>13</sup>C NMR (75 MHz, DMSO-*d*<sub>6</sub>) δ: 187.51 (C15), 175.80 (C1), 164.42 (C19), 155.51 (C5), 143.12 (C13), 133.62 (C21), 131.36 (C20), 130.80 (C18), 130.61 (C22), 129.60 (C8), 128.76 (C7, C9), 126.45 (C6, C10), 121.42 (C14), 109.32 (C23), 81.51 (C2), 72.62 (C16), 28.89 (C17), 25.67 (C3, C4), 18.05 (C11, C12). ESI-MS *m/z*: 379.1 [M-H]<sup>-</sup>. Anal. calcd. For C<sub>23</sub>H<sub>24</sub>O<sub>5</sub>: C, 72.61; H, 6.36; Found: C, 72.52; H, 6.28.

**(E)-2-(2-fluoro-4-(3-(4-(methylthio)phenyl)-3-oxoprop-1-en-1-yl)phenoxy)-2-methylpropanoic acid (5)**

Yield 44%; m.p. 118-120 °C; <sup>1</sup>H NMR (300 MHz, DMSO-*d*<sub>6</sub>) δ: 8.11 (d, *J* = 8.5 Hz, 2H), 7.99 – 7.77 (m, 3H), 7.71 – 7.65 (m, 1H), 7.41 – 7.33 (m, 2H), 6.99 (t, *J* = 8.6 Hz, 1H), 2.56 (s, 3H), 1.55 (s, 6H). <sup>13</sup>C NMR (75 MHz, DMSO-*d*<sub>6</sub>) δ: 197.37 (C13), 188.16 (C1), 174.79 (C6), 146.01 (C5), 145.87 (C11, C17), 134.22 (C14), 133.51 (C8), 129.52 (C15, C19), 129.14 (C16, C18), 125.38 (C10), 125.28 (C9, C12), 121.62 (C7), 81.07 (C2), 25.55 (C3, C4), 14.38 (C20). ESI-MS *m/z*: 373.1 [M-H]<sup>-</sup>. Anal. calcd. For C<sub>20</sub>H<sub>19</sub>FO<sub>4</sub>S: C, 64.16; H, 5.12; Found: C, 64.35; H, 5.26.

**(E)-2-(2-chloro-4-(3-(4-(methylthio)phenyl)-3-oxoprop-1-en-1-yl)phenoxy)-2-methylpropanoic acid (6)**

Yield 47%; m.p. 132-134 °C; <sup>1</sup>H NMR (300 MHz, DMSO-*d*<sub>6</sub>) δ: 8.18 – 8.09 (m, 3H), 7.96 – 7.85 (m, 1H), 7.78 – 7.61 (m, 2H), 7.39 (d, *J* = 8.6 Hz, 2H), 6.93 (d, *J* = 8.6 Hz, 1H), 2.56 (s, 3H), 1.58 (s, 6H). <sup>13</sup>C NMR (75 MHz, DMSO-*d*<sub>6</sub>) δ: 188.15 (C13), 174.79 (C1), 153.35 (C5), 146.02 (C11, C17), 142.48 (C14), 134.21 (C15, C19), 130.40 (C8), 129.55 (C9), 129.49 (C16, C18), 125.36 (C7), 124.69 (C6), 121.66 (C12), 118.01 (C10), 80.83 (C2), 25.55 (C3, C4), 14.39 (C20). ESI-MS *m/z*: 389.1 [M-H]<sup>-</sup>. Anal. calcd. For C<sub>20</sub>H<sub>19</sub>ClO<sub>4</sub>S: C, 61.46; H, 4.90; Found: C, 61.58; H, 4.76.

**General synthetic procedure for targets 7 and 8**

To a solution of **3d** (or **3e**) in acetonitrile was added  $K_2CO_3$  (3 equiv), and methyl bromoacetate (1.1 equiv). The mixture was stirred at room temperature for 12h. The mixture was filtered and the filtrate was concentrated to afford solid. The residue was purified by silica gel column chromatography to afford a white solid, which was dissolved in the mixed solvent of THF/MeOH/H<sub>2</sub>O (18 mL, 2:3:1), and added lithium hydroxide (1.5 equiv). After stirring at room temperature for 4 h, the volatiles were removed under reduced pressure. The residue was acidified with 1N hydrochloric acid solution and then filtered and the filter cake was washed with cold water (5 mL), dried in vacuum to afford a white powder. Recrystallization from 75% ethanol provides pure compound **7** (or **8**).

**(E)-2-(2-fluoro-4-(3-(4-(methylthio)phenyl)-3-oxoprop-1-en-1-yl)phenoxy)acetic acid (7)**

Yield 46%; m.p. 206-208 °C; <sup>1</sup>H NMR (300 MHz, DMSO-*d*<sub>6</sub>) δ: 13.23 (s, 1H), 8.11 (d, *J* = 8.5 Hz, 2H), 8.00 – 7.82 (m, 2H), 7.72 – 7.54 (m, 2H), 7.40 (d, *J* = 8.5 Hz, 2H), 7.15 (t, *J* = 8.7 Hz, 1H), 4.88 (s, 2H), 2.56 (s, 3H). <sup>13</sup>C NMR (75 MHz, DMSO-*d*<sub>6</sub>) δ: 188.16 (C11), 170.03 (C1), 151.67 (C4), 146.00 (C9, C15), 142.93 (C3), 134.24 (C12), 129.53 (C6), 129.13 (C13, C17), 127.20 (C14, C16), 125.38 (C7, C8), 121.51 (C10), 115.13 (C5), 65.45 (C2), 14.39 (C18). ESI-MS *m/z*: 345.1 [M-H]<sup>-</sup>. Anal. calcd. For C<sub>18</sub>H<sub>15</sub>FO<sub>4</sub>S: C, 62.42; H, 4.37; Found: C, 62.25; H, 4.23.

**(E)-2-(2-chloro-4-(3-(4-(methylthio)phenyl)-3-oxoprop-1-en-1-yl)phenoxy)acetic acid (8)**

Yield 41%; m.p. 203-205 °C; <sup>1</sup>H NMR (300 MHz, DMSO-*d*<sub>6</sub>) δ: 8.15 (d, *J* = 8.6 Hz, 2H), 7.99 – 7.84 (m, 2H), 7.76 – 7.58 (m, 1H), 7.48 – 7.33 (m, 3H), 7.11 (d, *J* = 8.7 Hz, 1H), 4.91 (s, 2H), 2.57 (s, 3H). <sup>13</sup>C NMR (75 MHz, DMSO-*d*<sub>6</sub>) δ: 189.07 (C11), 170.06 (C1), 153.58 (C3), 145.35 (C15), 142.85 (C9), 134.36 (C12), 128.95 (C6, C13, C17), 128.33 (C7), 127.45 (C14, C16), 127.34 (C5), 122.51 (C4), 121.32 (C10), 112.15 (C8), 65.47 (C2), 14.52 (C18). ESI-MS *m/z*: 361.1 [M-H]<sup>-</sup>. Anal. calcd. For C<sub>18</sub>H<sub>15</sub>ClO<sub>4</sub>S: C, 59.59; H, 4.17; Found: C, 59.43; H, 4.35.

**General synthetic procedure for targets 9 and 10**

To a solution of **3e** (or **3f**) in acetonitrile was added  $K_2CO_3$  (3 equiv), and methyl methyl 2-bromopropionate (1.1 equiv). The mixture was stirred at room temperature for 12h. The mixture was filtered and the filtrate was concentrated to afford solid. The residue was purified by silica gel column chromatography to afford a white solid, which was dissolved in the mixed solvent of

THF/MeOH/H<sub>2</sub>O (18 mL, 2:3:1), and added lithium hydroxide (1.5 equiv). After stirring at room temperature for 4 h, the volatiles were removed under reduced pressure. The residue was acidified with 1N hydrochloric acid solution, and then filtered and the filter cake was washed with cold water (5 mL), dried in vacuum to afford a white powder. Recrystallization from 75% ethanol provides pure compound **9** (or **10**).

**(E)-2-(2-chloro-4-(3-(4-(methylthio)phenyl)-3-oxoprop-1-en-1-yl)phenoxy)propanoic acid (9)**

Yield 35%; m.p. 150-152 °C; <sup>1</sup>H NMR (300 MHz, DMSO-*d*<sub>6</sub>) δ: 8.11 (d, *J* = 8.5 Hz, 2H), 7.96 – 7.80 (m, 2H), 7.76 – 7.57 (m, 2H), 7.39 (d, *J* = 8.5 Hz, 2H), 7.00 (d, *J* = 8.8 Hz, 1H), 4.99 (q, *J* = 6.7 Hz, 1H), 2.56 (s, 3H), 1.55 (d, *J* = 6.7 Hz, 3H). <sup>13</sup>C NMR (75 MHz, DMSO-*d*<sub>6</sub>) δ: 188.14 (C12), 173.00 (C1), 155.30 (C4), 145.95 (C16), 142.63 (C10), 134.25 (C13), 130.29 (C14, C18), 130.10 (C7), 129.54 (C8), 128.99 (C15, C17), 125.35 (C6), 122.54 (C5), 121.28 (C11), 114.47 (C9), 73.52 (C2), 18.72 (C3), 14.40 (C19). ESI-MS *m/z*: 375.2 [M-H]<sup>-</sup>. Anal. calcd. For C<sub>19</sub>H<sub>17</sub>ClO<sub>4</sub>S: C, 60.56; H, 4.55; Found: C, 60.34; H, 4.41.

**(E)-2-(2,6-dimethyl-4-(3-(4-(methylthio)phenyl)-3-oxoprop-1-en-1-yl)phenoxy)propanoic acid (10)**

Yield 40%; m.p. 132-134 °C; <sup>1</sup>H NMR (300 MHz, DMSO-*d*<sub>6</sub>) δ: 8.09 (d, *J* = 8.6 Hz, 2H), 7.87 – 7.73 (m, 1H), 7.66 – 7.50 (m, 3H), 7.39 (d, *J* = 8.6 Hz, 2H), 4.49 (q, *J* = 6.7 Hz, 1H), 2.55 (s, 3H), 2.28 (s, 6H), 1.42 (d, *J* = 6.7 Hz, 3H). <sup>13</sup>C NMR (75 MHz, DMSO-*d*<sub>6</sub>) δ: 188.24 (C14), 173.63 (C1), 157.39 (C4), 145.85 (C18), 143.97 (C12), 134.35 (C15), 131.50 (C16, C20), 130.30 (C17, C19), 130.16 (C7), 129.46 (C6, C8), 125.37 (C5, C9), 120.96 (C13), 77.45 (C2), 18.99 (C3), 17.25 (C10, C11), 14.40 (C21). ESI-MS *m/z*: 369.1 [M-H]<sup>-</sup>. Anal. calcd. For C<sub>21</sub>H<sub>22</sub>O<sub>4</sub>S: C, 68.09; H, 5.99; Found: C, 68.23; H, 5.85.

#### 4.2 Molecular docking

Molecular docking simulations of compounds **6** were performed using AutoDock vina1.1.2[36]. The crystal structures of PPAR $\alpha$  (PDB code: 3VI8) and PPAR $\delta$  (PDB code: 1GWX) were obtained from Protein Data Bank. Before the docking study, we conducted a re-dock study to verify the accuracy of the docking method. In the re-dock study of PPAR $\alpha$  and PPAR $\delta$ , the RMSDs (root-

mean-square-deviations) calculated by VMD 1.9.3 is 0.6718 and 1.601, respectively. These results show that our docking method and parameter settings are reliable in molecular docking simulations. After that, we have docked compound **6** with PPAR $\alpha$  and PPAR $\delta$ , and the docking pictures were drawn by Pymol 2.3.1.

#### ***4.3 Evaluation for PPAR $\alpha$ , PPAR $\gamma$ and PPAR $\delta$***

Detailed descriptions on transfection and cell-based evaluation for PPAR $\alpha$ , PPAR $\gamma$  and PPAR $\delta$  were given in our previously reported literature [22]. Briefly, HepG2 or HEK293 cells were transfected with pBIND-PPAR $\alpha$ , PPAR $\delta$  or PPAR $\gamma$  according to the manufacturer's protocol. After transfection, tested compounds were added and incubated for 18 h, then lysed with lysis buffer, and added Luciferase Assay Reagent II. The luciferase signals of firefly and renilla were measured using Dual Luciferase Reporter Assay System (Promega). EC<sub>50</sub> values were obtained from GraphPad 5.00 (San Diego, USA).

#### ***4.4 Animals and statistical analysis of the data***

Six weeks old male *ob/ob* mice were purchased from Model Animal Research Center of nanjing university (Jiangsu, China). All animals were acclimatized for 1 week before the experiments. The animal room was maintained under a constant 12 h light/black cycle with temperature at  $23 \pm 2$  °C and relative humidity  $50 \pm 10\%$  throughout the experimental period. Mice were allowed ad libitum access to standard pellets and water unless otherwise stated, and the vehicle used for drug administration was 0.5% sodium salt of Carboxy Methyl Cellulose aqueous solution for all animal studies. All animal experimental protocols were approved by the ethical committee at Guangdong Pharmaceutical University and conducted according to the Laboratory Animal Management Regulations in China and adhered to the Guide for the Care and Use of Laboratory Animals published by the National Institutes of Health (NIH Publication NO. 85-23, revised 2011).

Statistical analyses were performed using GraphPad InStat version 5.00 (San Diego, CA, USA). General effects were analyzed by using a one-way ANOVA with Tukey's multiple-comparison post hoc test.

#### ***4.5 Oral Glucose Tolerance Test in male ob/ob mice***

The male *ob/ob* mice were dosed once daily with the vehicle, GFT505 (10 mg/kg) or compound **6** (3, 10, and 20 mg/kg) by gavage administration for 5 days. Mice were dosed at fixed time daily, and OGTT was performed on day 6. Mice were fasted overnight prior to treatment with a single doses of vehicle, GFT505 or compound **6** and subsequently dosed orally with glucose aqueous solution (3 g/kg) after 30 min. Mice were bled via tail tip immediately before drug administration (-30 min), before glucose challenge (0 min), and at 30, 60 and 120 min post-dose and the blood glucose was measured by blood glucose test strips (SanNuo ChangSha, China).

### **Conflicts of interest**

The authors declare no conflict of interest. The authors are solely responsible for the content and results presented in this paper.

### **Acknowledgments**

This study was supported by the Guangdong Basic and Applied Basic Research Foundation (Grant 2019A1515011036), the National Natural Science Foundation of China (Grant 81803341), the Natural Science Foundation of Guangdong Province, China (Grant 2018A030313445), the Innovative strong school project of Guangdong Pharmaceutical University (Grant 2018KTSCX111), the projects of Guangzhou key laboratory of construction and application of new drug screening model systems (No. 201805010006) and Key Laboratory of New Drug Discovery and Evaluation of ordinary universities of Guangdong province (No. 2017KSYS002), the Innovation Team Projects in Universities of Guangdong Province (No. 2018KCXTD016).

**References**

- [1] R.A. DeFronzo, From the Triumvirate to the Ominous Octet: A New Paradigm for the Treatment of Type 2 Diabetes Mellitus, *Diabetes* 58 (2009) 773-795.
- [2] G. Danaei, M.M. Finucane, Y. Lu, G.M. Singh, M.J. Cowan, C.J. Paciorek, J.K. Lin, F. Farzadfar, Y.-H. Khang, G.A. Stevens, M. Rao, M.K. Ali, L.M. Riley, C.A. Robinson, M. Ezzati, C. Global Burden Metab Risk Factors, National, regional, and global trends in fasting plasma glucose and diabetes prevalence since 1980: systematic analysis of health examination surveys and epidemiological studies with 370 country-years and 2.7 million participants, *Lancet* 378 (2011) 31-40.
- [3] J.S. Skyler, Diabetes mellitus: pathogenesis and treatment strategies, *J. Med. Chem.* 47 (2004) 4113-4117.
- [4] O.J. Phung, J.M. Scholle, M. Talwar, C.I. Coleman, Effect of noninsulin antidiabetic drugs added to metformin therapy on glycemic control, weight gain, and hypoglycemia in type 2 diabetes, *JAMA* 303 (2010) 1410-1418.
- [5] S.A. Stein, E.M. Lamos, S.N. Davis, A review of the efficacy and safety of oral antidiabetic drugs, *Expert Opin Drug Saf* 12 (2013) 153-175.
- [6] Q.C. Zhang, C. Hastings, K. Johnson, E. Slaven, Metformin-Associated Lactic Acidosis Presenting Like Acute Mesenteric Ischemia, *J Emerg Med* (2019).
- [7] G.S. Wang, C. Hoyte, Review of Biguanide (Metformin) Toxicity, *J Intensive Care Med* (2018).
- [8] Z.-H. Zhao, Y.-C. Fan, Q. Zhao, C.-Y. Dou, X.-F. Ji, J. Zhao, S. Gao, X.-Y. Li, K. Wang, Promoter methylation status and expression of PPAR-gamma gene are associated with prognosis of acute-on-chronic hepatitis B liver failure, *Clin. Epigenet* 7 (2015).
- [9] F. Hong, S. Pan, Y. Guo, P. Xu, Y. Zhai, PPARs as Nuclear Receptors for Nutrient and Energy Metabolism, *Molecules (Basel, Switzerland)* 24 (2019).
- [10] B. Gross, M. Pawlak, P. Lefebvre, B. Staels, PPARs in obesity-induced T2DM, dyslipidaemia and NAFLD, *Nat Rev Endocrinol* 13 (2017) 36-49.
- [11] V. Chandra, P. Huang, Y. Hamuro, S. Raghuram, Y. Wang, T.P. Burris, F. Rastinejad, Structure of the intact PPAR- $\gamma$ -RXR- $\alpha$  nuclear receptor complex on DNA, *Nature* 456 (2008) 350-356.
- [12] H.E. Xu, M.H. Lambert, V.G. Montana, D.J. Parks, S.G. Blanchard, P.J. Brown, D.D. Sternbach, J.M. Lehmann, G.B. Wisely, T.M. Willson, Molecular recognition of fatty acids by peroxisome proliferator-activated receptors, *Mol. Cell* 3 (1999) 397-403.
- [13] S. Francque, A. Verrijken, S. Caron, J. Prawitt, R. Paumelle, B. Derudas, P. Lefebvre, M.R. Taskinen, W. Van Hul, I. Mertens, G. Hubens, E. Van Marck, P. Michielsen, L. Van Gaal, B. Staels, PPAR $\alpha$  gene expression correlates with severity and histological treatment response in patients with non-alcoholic steatohepatitis, *J. Hepatol.* 63 (2015) 164-173.
- [14] K.H. Liss, B.N. Finck, PPARs and nonalcoholic fatty liver disease, *Biochimie* 136 (2017) 65-74.
- [15] H. Kim, M. Haluzik, Z. Asghar, D. Yau, J.W. Joseph, A.M. Fernandez, M.L. Reitman, S. Yakar, B. Stannard, L. Heron-Milhavet, M.B. Wheeler, D. LeRoith, Peroxisome proliferator-activated receptor-alpha agonist treatment in a transgenic model of type 2 diabetes reverses the lipotoxic state and improves glucose homeostasis, *Diabetes* 52 (2003) 1770-1778.
- [16] Rosenson, R. S, Fenofibrate: treatment of hyperlipidemia and beyond, *Expert Rev Cardiovasc Ther* 6 (2008) 1319-1330.
- [17] Y.X. Wang, C.H. Lee, S. Tjep, R.T. Yu, J.Y. Ham, H.J. Kang, R.M. Evans, Peroxisome-proliferator-activated receptor delta activates fat metabolism to prevent obesity, *Cell* 113 (2003) 159-170.
- [18] X. Palomer, E. Barroso, J. Pizarro-Delgado, L. Pena, G. Botteri, M. Zarei, D. Aguilar, M. Montori-

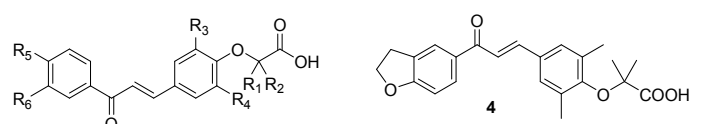
- Grau, M. Vazquez-Carrera, PPAR beta/delta: A Key Therapeutic Target in Metabolic Disorders, *Int. J. Mol. Sci.* 19 (2018).
- [19] T. Tanaka, J. Yamamoto, S. Iwasaki, H. Asaba, H. Hamura, Y. Ikeda, M. Watanabe, K. Magoori, R.X. Ioka, K. Tachibana, Y. Watanabe, Y. Uchiyama, K. Sumi, H. Iguchi, S. Ito, T. Doi, T. Hamakubo, M. Naito, J. Auwerx, M. Yanagisawa, T. Kodama, J. Sakai, Activation of peroxisome proliferator-activated receptor delta induces fatty acid beta-oxidation in skeletal muscle and attenuates metabolic syndrome, *Proc. Natl. Acad. Sci. U. S. A.* 100 (2003) 15924-15929.
- [20] D.L. Sprecher, C. Massien, G. Pearce, A.N. Billin, I. Perlstein, T.M. Willson, D.G. Hassall, N. Ancellin, S.D. Patterson, D.C. Lobe, T.G. Johnson, Triglyceride:high-density lipoprotein cholesterol effects in healthy subjects administered a peroxisome proliferator activated receptor delta agonist, *Arterioscler., Thromb., Vasc. Biol.* 27 (2007) 359-365.
- [21] T. Adhikary, A. Wortmann, T. Schumann, F. Finkernagel, S. Lieber, K. Roth, P.M. Toth, W.E. Diederich, A. Nist, T. Stiewe, L. Kleinesudeik, S. Reinartz, S. Muller-Brusselbach, R. Muller, The transcriptional PPARbeta/delta network in human macrophages defines a unique agonist-induced activation state, *Nucleic Acids Res.* 43 (2015) 5033-5051.
- [22] Z. Li, Z. Zhou, F. Deng, Y. Li, D. Zhang, L. Zhang, Design, synthesis, and biological evaluation of novel pan agonists of FFA1, PPARgamma and PPARdelta, *Eur. J. Med. Chem.* 159 (2018) 267-276.
- [23] Z. Li, Y. Chen, Z. Zhou, L. Deng, Y. Xu, L. Hu, B. Liu, L. Zhang, Discovery of first-in-class thiazole-based dual FFA1/PPARdelta agonists as potential anti-diabetic agents, *Eur. J. Med. Chem.* 164 (2019) 352-365.
- [24] Z. Li, L. Hu, X. Wang, Z. Zhou, L. Deng, Y. Xu, L. Zhang, Design, synthesis, and biological evaluation of novel dual FFA1 (GPR40)/PPARdelta agonists as potential anti-diabetic agents, *Bioorg. Chem.* 92 (2019) 103254.
- [25] Z. Li, C. Liu, Z. Zhou, L. Hu, L. Deng, Q. Ren, H. Qian, A novel FFA1 agonist, CPU025, improves glucose-lipid metabolism and alleviates fatty liver in obese-diabetic (ob/ob) mice, *Pharmacol. Res.* 153 (2020) 104679.
- [26] Y. Chen, Q. Ren, Z. Zhou, L. Deng, L. Hu, L. Zhang, Z. Li, HWL-088, a new potent free fatty acid receptor 1 (FFAR1) agonist, improves glucolipid metabolism and acts additively with metformin in ob/ob diabetic mice, *Br. J. Pharmacol.* (2020).
- [27] M. Ahmadian, J.M. Suh, N. Hah, C. Liddle, A.R. Atkins, M. Downes, R.M. Evans, PPAR gamma signaling and metabolism: the good, the bad and the future, *Nat. Med.* 19 (2013) 557-566.
- [28] G. Derosa, A. Sahebkar, P. Maffioli, The role of various peroxisome proliferator-activated receptors and their ligands in clinical practice, *J Cell Physiol* 233 (2018) 153-161.
- [29] A.Z. Mirza, Althagafi, II, H. Shamshad, Role of PPAR receptor in different diseases and their ligands: Physiological importance and clinical implications, *Eur. J. Med. Chem.* 166 (2019) 502-513.
- [30] F. Hong, P. Xu, Y. Zhai, The Opportunities and Challenges of Peroxisome Proliferator-Activated Receptors Ligands in Clinical Drug Discovery and Development, *Int. J. Mol. Sci.* 19 (2018).
- [31] B. Cariou, B. Charbonnel, B. Staels, Thiazolidinediones and PPARgamma agonists: time for a reassessment, *Trends Endocrinol. Metab.* 23 (2012) 205-215.
- [32] A.M. Lincoff, J.C. Tardif, G.G. Schwartz, S.J. Nicholls, L. Ryden, B. Neal, K. Malmberg, H. Wedel, J.B. Buse, R.R. Henry, A. Weichert, R. Cannata, A. Svensson, D. Volz, D.E. Grobbee, Effect of aleglitazar on cardiovascular outcomes after acute coronary syndrome in patients with type 2 diabetes mellitus: the AleCardio randomized clinical trial, *JAMA* 311 (2014) 1515-1525.
- [33] M.Á. Herrera-Rueda, H. Tlahuext, P. Paoli, A. Giacomani-Martínez, J.C. Almanza-Pérez, H. Pérez-

Sánchez, A. Gutiérrez-Hernández, F. Chávez-Silva, E.A. Dominguez-Mendoza, S. Estrada-Soto, Design, synthesis, in vitro, in vivo and in silico pharmacological characterization of antidiabetic N-Boc-L-tyrosine-based compounds, *Biomed Pharmacother* 108 (2018) 670-678.

[34] G. Navarrete-Vázquez, H. Torres-Gómez, S. Hidalgo-Figueroa, J.J. Ramírez-Espinosa, S. Estrada-Soto, J.L. Medina-Franco, I. León-Rivera, F.J. Alarcón-Aguilar, J.C. Almanza-Pérez, Synthesis, in vitro and in silico studies of a PPAR $\gamma$  and GLUT-4 modulator with hypoglycemic effect, *Bioorg Med Chem Lett* 24 (2014) 4575-4579.

[35] B. Colín-Lozano, S. Estrada-Soto, F. Chávez-Silva, A. Gutiérrez-Hernández, L. Cerón-Romero, A. Giacomán-Martínez, J.C. Almanza-Pérez, E. Hernández-Núñez, Z. Wang, X. Xie, Design, synthesis and in combo antidiabetic bioevaluation of multitarget phenylpropanoic acids, *Molecules* 23 (2018) 340.

[36] O. Trott, A.J. Olson, AutoDock Vina: improving the speed and accuracy of docking with a new scoring function, efficient optimization, and multithreading, *J. Comput. Chem.* 31 (2010) 455-461.

**Table 1:** *In vitro* activities of the human PPARs <sup>a</sup>


Compd.	R <sub>1</sub>	R <sub>2</sub>	R <sub>3</sub>	R <sub>4</sub>	R <sub>5</sub>	R <sub>6</sub>	<i>h</i> PPAR $\alpha$	<i>h</i> PPAR $\gamma$	<i>h</i> PPAR $\delta$
							EC <sub>50</sub> ( $\mu$ M)	EC <sub>50</sub> ( $\mu$ M)	EC <sub>50</sub> ( $\mu$ M)
<b>GW7647</b>							0.013	ND	ND
<b>Rosiglitazone</b>							ND	0.115	ND
<b>GW0742</b>							ND	ND	0.021
<b>GFT505</b>	Me	Me	Me	Me	MeS	H	0.355	3.622	0.253
<b>1</b>	Me	Me	Me	Me	MeO	F	0.627	1.374	0.557
<b>2</b>	Me	Me	Me	Me	D <sub>3</sub> CO	F	0.735	2.183	0.528
<b>3</b>	Me	Me	Me	Me	D <sub>3</sub> CS	F	0.503	4.715	0.396
<b>4</b>							1.257	0.926	0.739
<b>5</b>	Me	Me	F	H	MeS	H	0.871	> 10	0.516
<b>6</b>	Me	Me	Cl	H	MeS	H	0.468	> 10	0.362
<b>7</b>	H	H	F	H	MeS	H	6.285	> 10	3.195
<b>8</b>	H	H	Cl	H	MeS	H	3.274	> 10	2.509
<b>9</b>	Me	H	Cl	H	MeS	H	0.583	> 10	0.381
<b>10</b>	Me	H	Me	Me	MeS	H	0.516	5.625	0.437

<sup>a</sup> EC<sub>50</sub> value represent the mean of three determinations, which is the concentration giving 50% of the maximal activity determined for the tested compound.

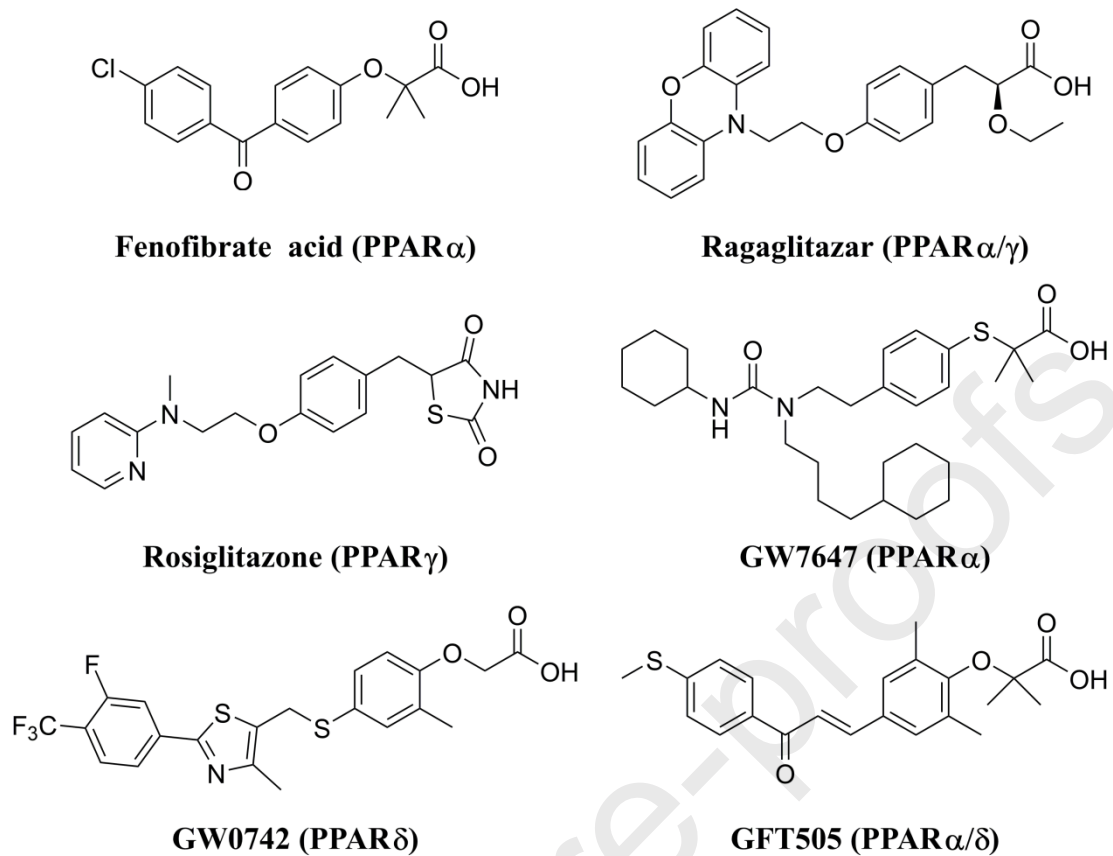


**Figure 1:** Structure of PPARs agonists.

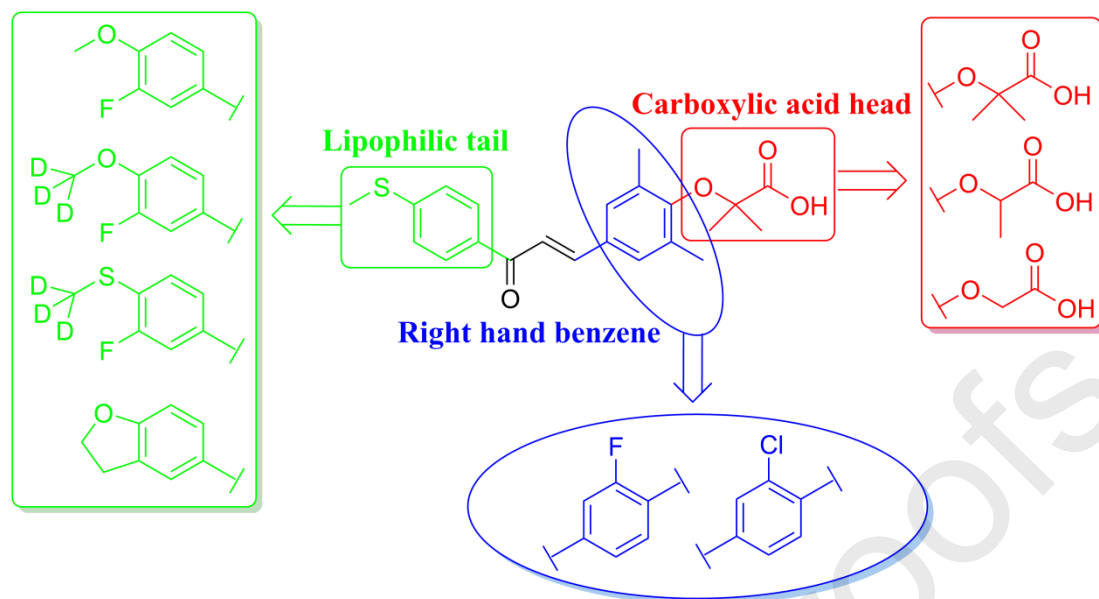


**Figure 2:** The design strategy for the modification of GFT505.



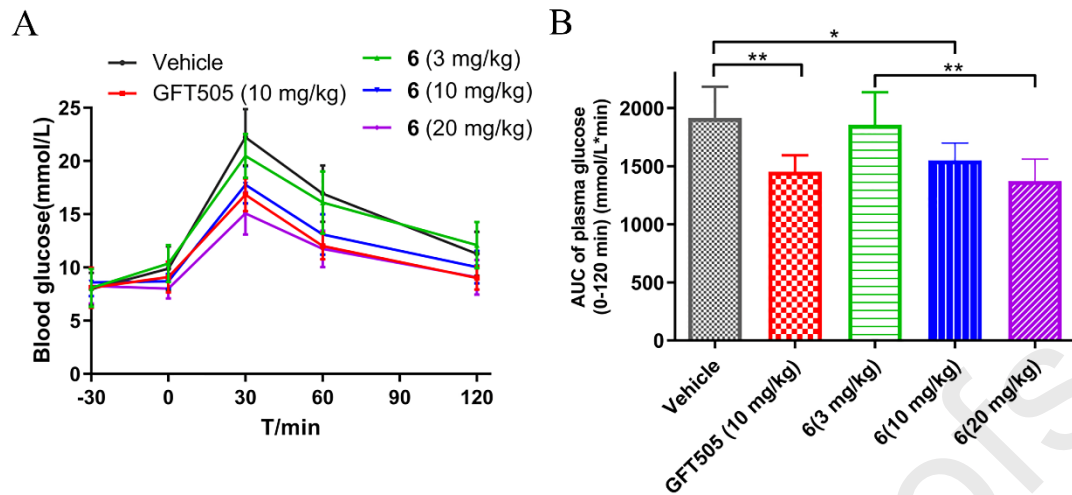
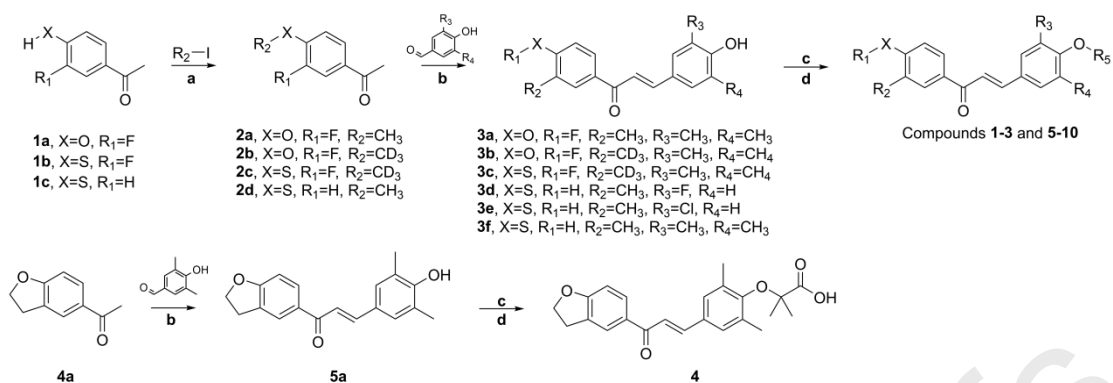


**Figure 4:** Effects of compound **6** on plasma glucose levels and corresponding  $AUC_{0-120\text{min}}$  of glucose during an OGTT in fasting *ob/ob* mice after five days treatment. GFT505, compound **6**, or vehicle was orally administered to *ob/ob* mice once daily for 5 days, and the OGTT was determined on treatment day 6. Values are mean  $\pm$  SD ( $n = 6$  per group).  $*p \leq 0.05$  and  $**p \leq 0.01$  was analyzed using a one-way ANOVA with Tukey's multiple-comparison post hoc test.

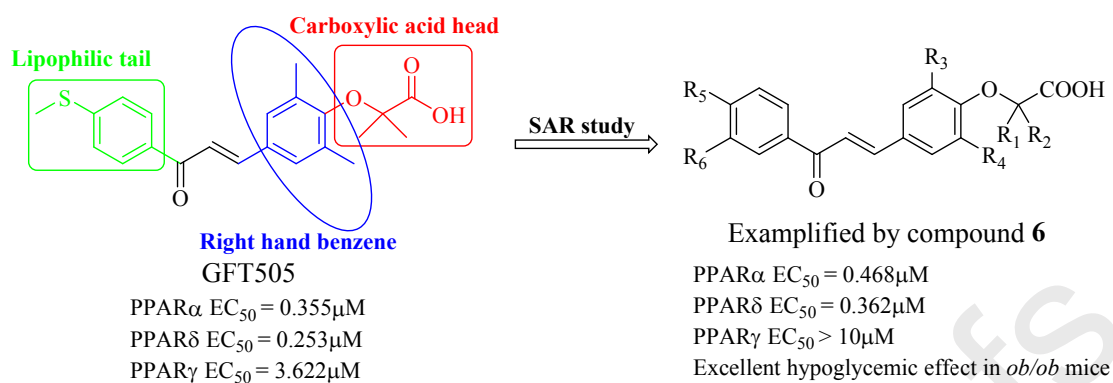


**Scheme 1:** Synthesis of target compounds **1-10**. Reagent and condition: (a) K<sub>2</sub>CO<sub>3</sub>, KI, acetonitrile, r.t., 12h; (b) H<sub>2</sub>SO<sub>4</sub>, MeOH, r.t., 16h; (c) Methyl 2-bromo-2-methylpropanoate (methyl 2-bromopropionate, or methyl bromoacetate), K<sub>2</sub>CO<sub>3</sub>, KI, acetonitrile, 50 °C, 16h; (d) LiOH·H<sub>2</sub>O, THF/MeOH/H<sub>2</sub>O, r.t., 4h.

### Highlights

1. Compound **6** shows higher selectivity to PPAR $\alpha/\delta$  and lower agonistic activity on PPAR $\gamma$ .
2. Compound **6** exerts dose-dependent anti-diabetic effects in *ob/ob* mice.
3. Compound **6** reveals similar potency to GFT505, the most advanced candidate in this field.
4. The obtained SAR in this study might help us to explore better PPAR $\alpha/\delta$  agonist.

## Graphical Abstract



From the SAR study based on GFT505, a dual PPAR $\alpha/\delta$  agonist compound **6** was identified, which has lower agonistic activity on PPAR $\gamma$  and exerted excellent hypoglycemic effect in *ob/ob* mice.

Journal Pre-proofs

**Conflict of interest**

The authors declare no competing financial interest.

Journal Pre-proofs